Slow progressive degeneration of nigral dopaminergic neurons in postnatal *Engrailed* mutant mice

Paola Sgadò*, Lavinia Albéri*, Daniel Gherbassi*, Sherri L. Galasso†, Geert M. J. Ramakers‡, Kambiz N. Alavian*, Marten P. Smidt‡, Richard H. Dyck†, and Horst H. Simon*§

*Interdisciplinary Center for Neuroscience, Department of Neuroanatomy, Ruprecht-Karls Universität Heidelberg, 69120 Heidelberg, Germany; ‡Rudolf Magnus Institute of Neuroscience, Department of Pharmacology and Anatomy, University Medical Centre, 3584 CG Utrecht, The Netherlands; and †Departments of Psychology and Cell Biology and Anatomy, Hotchkiss Brain Institute, University of Calgary, Calgary, AB, Canada T2N 1N4

Edited by Richard D. Palmiter, University of Washington School of Medicine, Seattle, WA, and approved August 21, 2006 (received for review March 15, 2006)

The homeobox transcription factors *Engrailed-1* and *Engrailed-2* are required for the survival of mesencephalic dopaminergic neurons in a cell-autonomous and gene-dose-dependent manner. Because of this requirement, the cells die by apoptosis when all four alleles of the *Engrailed* genes are genetically ablated (*En1*−/−; *En2*−/−). In the present study, we show that viable and fertile mice, heterozygous null for *Engrailed-1* and homozygous null for *Engrailed-2* (*En1*+/−;*En2*−/−), have an adult phenotype that resembles key pathological features of Parkinson's disease. Specifically, postnatal mutant mice exhibit a progressive degeneration of dopaminergic neurons in the substantia nigra during the first 3 mo of their lives, leading to diminished storage and release of dopamine in the caudate putamen, motor deficits similar to akinesia and bradykinesia, and a lower body weight. This genetic model may provide access to the molecular etiology for Parkinson's disease and could assist in the development of novel treatments for this neurodegenerative disorder.

dopamine | midbrain | mouse mutant | neurodegenerative disease | substantia nigra

Mesencephalic dopaminergic (mesDA) neurons are the main source of dopamine in the mammalian central nervous system (1). They are located in three distinct nuclei, the substantia nigra pars compacta (SN), the ventral tegmentum (VTA), and the retrorubral field (RRF). Their main innervation targets are the basal ganglia, where they play a major role in controlling emotion, motivation, and motor behavior (2, 3), recognized by their involvement in schizophrenia, addiction, and most prominently in Parkinson's disease (PD; ref. 4). PD is a multisystemic degenerative disorder of the central and peripheral nervous systems. Its hallmark is the progressive degeneration of DA neurons in the SN. The clinical symptoms are resting tremor; muscular rigidity; postural instability; hyposomia; a positive response to the application of L-3,4-dihydroxyphenylalanine (L-DOPA); and the presence of cytoplasmatic inclusions (Lewy bodies) in postmortem brains (5). Additionally, PD patients are often characterized by weight loss starting before diagnosis and continuing with disease progression (6, 7).

The homeodomain transcription factors *Engrailed-1* and *-2* (*En1* and *En2*) are expressed by all mesDA neurons soon after differentiation and then continuously into adulthood. They are cell-autonomously and in a gene-dose-dependent manner required for the survival of this neuronal population, leading to the complete loss of the cells in mutant mice homozygous null for both genes (*En1*−/−;*En2*−/−; refs. 8 and 9). In their function as survival factors for mesDA neurons, the two genes are redundant and can compensate for each other (9, 10). The single-null mutants for either *En1* (*En1*−/−) or *En2* (*En2*−/−) show no significant alterations in the organization of the mesDA system at birth, but the mice with genotypes intermediate to the single and double mutants are distinctively different from each other. Whereas *En1*−/−;*En2*+/− mice die at postnatal day 0 (P0) and exhibit a large loss of mesDA neurons, *En1*+/−; *En2*−/− (En^{HT} hereafter) mice are viable and fertile and show a wild-type mesDA phenotype at birth.

Results

Specific Loss of Nigral Dopaminergic Neurons in *Engrailed* Mutant Mice. To determine the role of the *Engrailed* genes in mature animals, we examined the mesDA system in mice with different *Engrailed* genotypes at various postnatal ages. In accord with our previous reports, *En1*−/−, *En1*−/−;*En2*+/−, and *En1*−/−; *En2*−/− mice die at birth (8, 9) and show a gene-dose-dependent reduction of mesDA neurons (9). Mice of other *Engrailed* genotypes are viable and fertile. Among these, *En1*+/−, *En1*+/−;*En2*+/−, *En2*+/−, and *En2*−/− mice displayed a wild-type-like distribution of the neurons at all ages examined (data not shown; for *En2*−/−; see Fig. 1 *E* and *F*). In contrast, En^{HT} mice showed a specific loss of DA neurons in the SN (Fig. 1*E′*), whereas the VTA and RRF were unaffected (Fig. 1*F′*). Because the distribution of mesDA neurons was normal in *En2*−/− mice, we continued our analysis using *En2*−/− mice as control littermates. By using stereological methods (11), we counted the tyrosine hydroxylase (TH)-positive cell bodies in the adult SN, VTA, and RRF separately (12). These counts showed that *En2*−/− mice were equivalent to wild-type C57/Bl6 (data not shown), whereas the number of nigral DA neurons in En^{HT} mutants was, on average, 67.2% lower (Fig. 1*I*). In contrast, no significant difference between genotypes was found in VTA and RRF (Fig. 1*J*).

To determine the age at which neuronal degeneration sets in, we extended our analysis to mice of different postnatal ages starting at birth. At postnatal day 0 (P0), the mesDA system of En^{HT} mice was unaltered, neither the distribution of the cells (Fig. 1 *A* and *A′*) nor their numbers (Fig. 1*G*) were significantly different from their *En2*−/− littermate controls. In total, we counted 26,349 ± 805 and 24,715 ± 1,734 TH-positive neurons in the ventral midbrain of En^{HT} and *En2*−/− mice, respectively; separated into individual nuclei, we found 5,582 ± 384 and 5,223 ± 464 in the SN, 17,302 ± 405 and 15,733 ± 1,163 in the VTA, and 3,465 ± 225 and 3,759 ± 525 in the RRF, respectively. As in wild-type mice, both genotypes showed a

Author contributions: P.S., R.H.D., and H.H.S. designed research; P.S., L.A., D.G., S.L.G., G.M.J.R., and K.N.A. performed research; P.S., D.G., G.M.J.R., M.P.S., R.H.D., and H.H.S. analyzed data; and R.H.D. and H.H.S. wrote the paper.

The authors declare no conflict of interest.

Abbreviations: mesDA, mesencephalic dopaminergic; SN, substantia nigra pars compacta; VTA, ventral tegmentum; RRF, retrorubral field; PD, Parkinson's disease; TH, tyrosine hydroxylase; CPu, caudate putamen; P*n*, postnatal day *n*.

§To whom correspondence should be addressed. E-mail: horst.simon@urz.uni-heidelberg.de.

© 2006 by The National Academy of Sciences of the USA

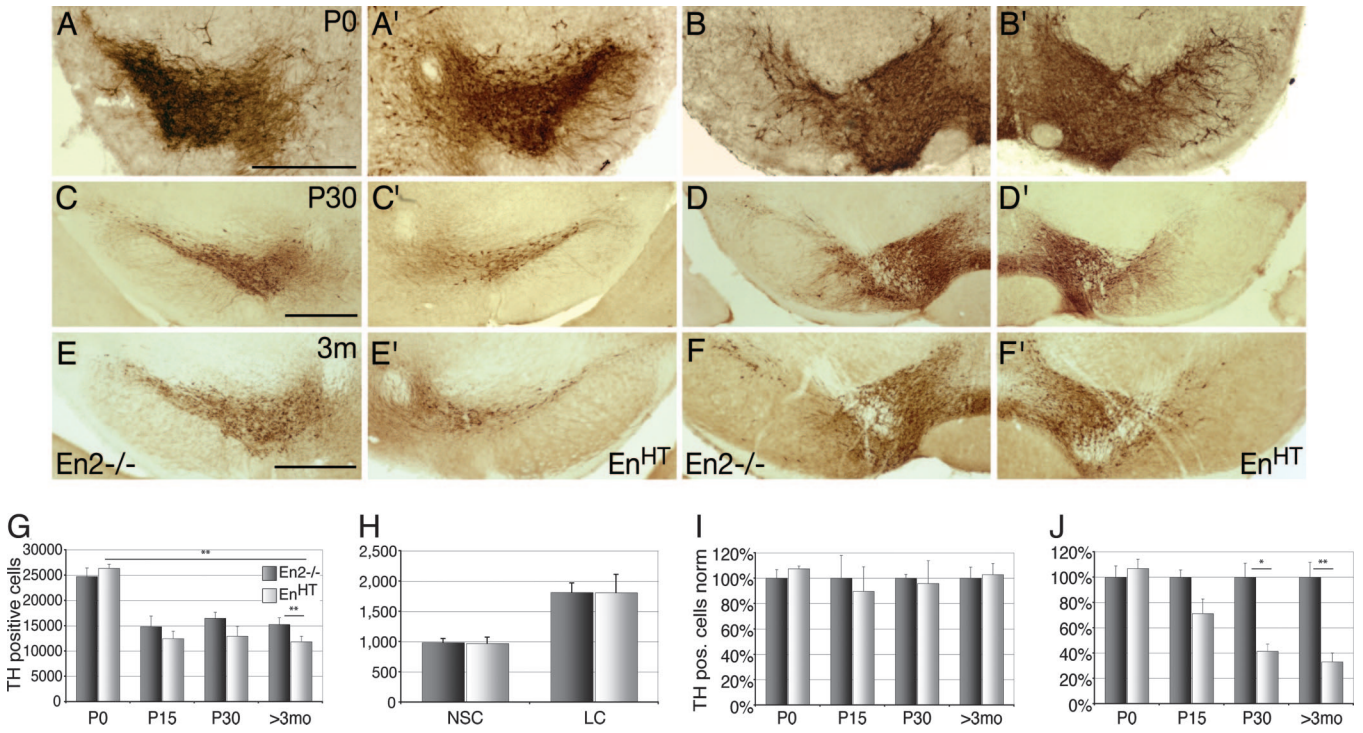

Fig. 1. Gradual postnatal loss of DA neuron in substantia nigra. (*A–F* and *A′–F′*) TH immunostaining on coronal brain section at P0 (*A*, *A′*, *B*, and *B′*), P30 (*C*, *C′*, *D*, and *D′*), and 3 mo (*E*, *E′*, *F*, and *F′*) of *En2*−/− and *En1*+/*tLZ*;*En2*−/− (*En*^{HT}) mouse mutants on the level of the substantia nigra (*A*, *A′*, *C*, *C′*, *E*, and *E′*) and the VTA (*B*, *B′*, *D*, *D′*, *F*, and *F′*). (*G–J*) Cell count of DA neurons in ventral midbrain (*G*, *I*, and *J*) and noradrenergic neurons in locus coeruleus (LC) and nucleus subcoeruleus (NSC) (*H*) ($n \geq 4$ for ages <3 mo; $n = 12$ for 3 mo and older). (*I*) VTA and RRF. (J) SN. (Error bars, standard error; *, $P < 0.01$; **, $P < 0.001$.) (Scale bars: 500 μm.)

decline in the numbers of mesDA neurons in the next 14 days (13); however, in the *En*^{HT} mice, this normal cell death overlaps with an additional genotype-associated loss of TH-positive cells reaching in total 16% at P15 (12,463 ± 1,496 in *En*^{HT} mice and 14,819 ± 2,109 in *En2*−/− control littermates; $P = 0.05$). In *En2*−/− mice, like in wild type, the numbers of mesDA neurons stabilized at this age. In the *En*^{HT} mice, however, the numbers continued to decrease until ≈3 mo after birth. From this age onward, the mutants had on average 32.6% fewer mesDA neurons than their *En2*−/− littermate controls (11,226 ± 935 for *En*^{HT} vs. 16,645 ± 1,786 for *En2*−/− mice; $P = 0.006$; Fig. 1*G*). Separate counts of SN, VTA, and RRF revealed that, at all ages (the oldest animal counted was 22 mo), cell loss was restricted to the SN (Fig. 1 *I* and *J*). In particular, the average number of DA neurons was 1,882 ± 708 and 6,115 ± 1,008 (−69.2 ± 11.6%, $P = 0.002$) in the SN and 9,766 ± 1,471 and 10,530 ± 1,234 in VTA and RRF of *En*^{HT} and *En2*−/− mice, respectively. (For a two-factorial ANOVA considering genotype and age, see *Supporting Text*, which is published as supporting information on the PNAS web site.) During the phase of cell loss, the mutants showed a high variance between individuals of the same age and sometimes even an asymmetric cell loss between the left and right hemispheres.

Data from our previous prenatal *in vivo* and *in vitro* studies had demonstrated that loss of mesDA neurons in *Engrailed* double-mutant embryos is a cell-autonomous function of the two transcription factors and not a result of deficiencies in the surrounding tissue (8, 14). To provide evidence that the *En*^{HT} phenotype also reflects a cell-autonomous function of *En1* and *En2*, we examined the noradrenergic neurons of the locus coeruleus in the mutants. These neurons do not express the *Engrailed* genes but depend on them for their development during embryogenesis (14), suggesting they are sensitive to morphological alterations in mid- and hindbrain. We found that neither the locus coeruleus nor the neighboring nucleus subcoeruleus was affected in *En*^{HT} mutants. In particular, we counted 1,809 ± 302 and 1,813 ± 156 noradrenergic neurons in the locus coeruleus and 969 ± 101 and 984 ± 65 in the nucleus subcoeruleus of *En*^{HT} and *En2*−/− animals, respectively (Fig. 1*H*).

It was possible that nigral DA neurons were not detectable in *En*^{HT} mice by immunolabeling against TH due to a change of their neurotransmitter phenotype. To elaborate on this possibility, we first investigated whether there were signs of cell death in nigral DA neurons; during the postnatal stages, they were most rapidly disappearing but were beyond the age of naturally occurring developmental cell death due to a glial cell-derived neurotrophic factor requirement (15). In the SN of P20 *En*^{HT} mutants, we typically detected ≈12–15 very small rounded TH-positive cell bodies, which were labeled against activated caspase-3 and showed pyknotic nuclei (Fig. 2 *A–C*). In the littermate control, the amount of TH-positive apoptotic figures was never more than three. Despite the presence of these apoptotic cells, we could not detect signs of activated astrocytes when using a glial fibrillary acidic protein antibody (data not shown). Second, we examined the expression pattern of seven additional genes expressed by mesDA neurons: *Pitx3*, *Pbx1*, *Aadc*, *Ahd2*, *Ret*, α-*Synuclein*, and γ-*Synuclein* (8, 16–18). Third, we stained against the *En1* reporter β-Gal (19) and compared *En*^{HT} with *En1*+/*tLZ*;*En2*+/+ mice. Fourth, we performed a Nissl staining, which is often used in model systems for PD. The expression analysis and histological stain revealed a normal distribution of neurons in the VTA and RRF and a loss of cell bodies in the SN comparable with that seen after TH immunohistochemistry (for a selection of these markers, see Fig. 2 *D–G*). Furthermore, to investigate whether the loss of nigral DA neurons is a result of a general morphological alteration, which we could not detect with Nissl staining, we analyzed the

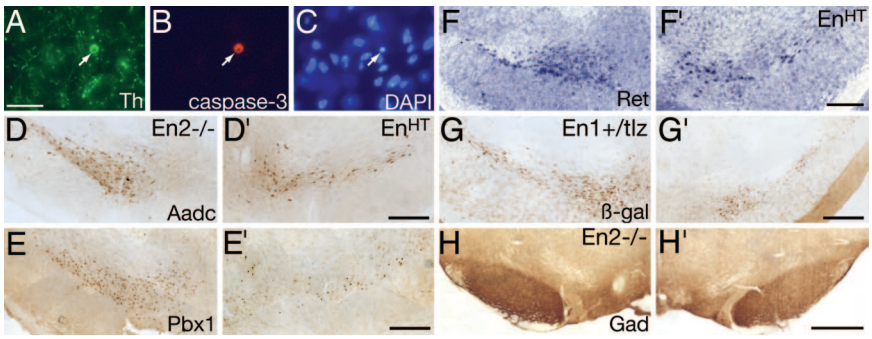

Fig. 2. Cell loss by apoptosis and no change in neurotransmitter phenotype. (*A*, *B*, and *C*) Coronal section at level of SN of P20 En^{HT} mouse stained against TH (green), activated caspase-3 (red), and DAPI (blue). The nigral DA neuron shows signs of apoptosis, a small rounded cell body, activated caspase-3, and a pyknotic nucleus (arrows). (*D–H*) Immunostaining against aromatic amino acid decarboxylase (Aadc) (*D*), Pbx1 (*E*), the *En1*-reporter β-Gal (*G*), and glutamate decarboxylase (Gad; *H*), and *in situ* hybridization against *Ret* (*F*), all on adult coronal brain sections of *En2*−/− (*D–F*, *H*), *En1*+/*tLZ*;*En2*−/− (En^{HT}) (*D′–H′*) and *En1*+/*tLZ* mice (*G*). Aadc, Pbx1, *Ret*, and β-Gal expression reveal all loss of nigral DA neurons in En^{HT} mice, whereas the Gad staining is the same in both genotypes (*H*). [Scale bars (*A–C*): 20 μm; (*D–H*): 500 μm.]

GABAergic population in the SN, which is located just ventral to nigral DA neurons and does not express *En1* or *En2* (20, 21). The GABAergic cell bodies and axons were normal in En^{HT} mice (Fig. 2*H*). Together, the immunohistochemical analysis and the histological stain show that nigral DA neurons of En^{HT} mice die by apoptosis and do not convert their neurotransmitter phenotype. Furthermore, the En1taulacZ expression pattern in an *En2* wild-type background (*En1*+/*tLZ*;*En2*+/+; Fig. 2*G*) revealed that the functional deletion of one *En1* allele is necessary but not sufficient to cause the loss of nigral DA neurons, and that *En2* also plays an essential role.

Molecular Changes in Basal Ganglia of En^{HT} Mice. Because deficiencies in the nigral DA system are associated with defects in their main innervation target, the caudate putamen (CPu), we investigated adult En^{HT} mice (>3 mo) for anatomical and molecular changes in the CPu. Despite the loss of almost 70% of nigral DA neurons, we did not see marked differences in the density of TH-positive terminals by immunohistochemistry (Fig. 3 *A* and *B*). To obtain a more accurate picture, we measured dopamine levels by HPLC. We found that the amount of dopamine in the striatum was significantly lower in En^{HT} mice (−38.9 ± 5.1%, $P = 0.001$) than in their *En2*−/− littermate controls (Fig. 3*C*). Furthermore, when we measured dopamine release in striatal slices by fast-scan cyclic voltametry (22), the amount of dopamine discharged upon a defined stimulus in the CPu was 21% lower in slices from En^{HT} animals (3.0 ± 0.28 and 3.8 ± 0.23 μM; $P = 0.001$ for En^{HT} and *En2*−/− mice, respectively). As expected from the cell counts, the dopamine release in the nucleus accumbens, which is innervated by VTA neurons, was unaltered (Fig. 3*D*).

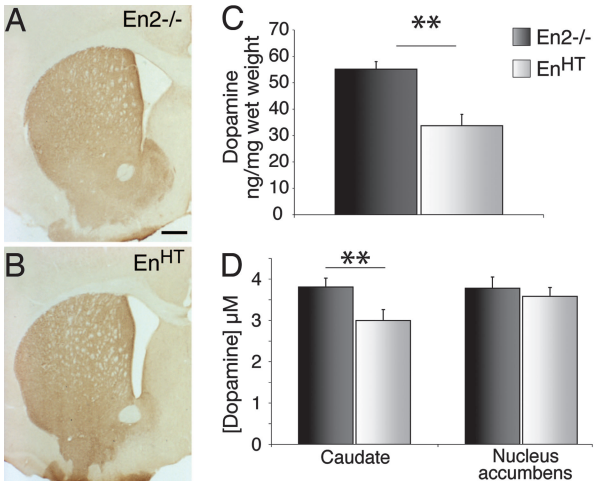

Fig. 3. Molecular changes in dorsal striatum. (*A* and *B*) TH immunostaining of basal ganglia showing no significant difference between genotypes. (*C*) Dopamine content in the dorsal striatum measured by HPLC ($n = 6$). (*D*) Dopamine release measured by cyclic voltametry ($n = 6$). (Scale bars: 500 μm; error bars, standard error; **, $P < 0.001$.)

A loss of DA innervation to the CPu had been shown to result in molecular changes in GABAergic output circuits (23). We therefore measured the expression levels of genes specific to the direct (*substance P* and *dynorphin*) and indirect pathways (*dopamine receptor 2*), All three genes were expressed significantly lower in En^{HT} than in *En2*−/− mice (53.1 ± 11.8%, $P = 0.011$; 55.2 ± 8.1%, $P = 0.003$, and 54.3 ± 6.3%, $P = 0.001$, respectively; $n \geq 8$). Taken together, these data demonstrate that the loss of DA neurons in the SN results in diminished storage and release of dopamine in the CPu and in concomitant molecular changes in GABAergic neurons deprived of that input.

Motor Performance in En^{HT} Mice. To determine the behavioral consequences in En^{HT} mice, we conducted a battery of tests that evaluate motor coordination, strength, balance, and locomotion. Some of these tests had previously been used to assess motor performance in rodent models for PD. Specifically, the mice were assessed in the following tests: open field, hang and grid performances, swimming, horizontal ladder, rotorod, stride, and cylinder (24–27). In addition, we examined the mice on two tasks that have cognitive components associated with them: the Morris water task and the elevated plus maze. It had previously been shown that the loss of *En2* causes alterations in the cerebellar organization (28) and an impairment of motor learning performance (29). Therefore, to limit our analysis to behavioral changes that may be associated with the loss of nigral DA neurons, we compared En^{HT} mice to their *En2*−/− littermates and not to wild type. Furthermore, because we did not observe any change in the numbers of nigral DA neurons after 3 mo of age (Fig. 1*i*), we chose to conduct the tests in animals of 8 mo and again at 18 mo of age to evaluate whether they exhibited an age-related decline in performance. The swimming performance and horizontal ladder tests were adopted only after the tests at 8 mo had been completed.

En^{HT} mice were impaired, relative to their *En2*−/− littermates, in four of the 10 tests that we used (Fig. 4). In the open field test, a general assessment of locomotor and exploratory behavior, En^{HT} mice were not impaired at 8 mo; however, by 18 mo of age, they

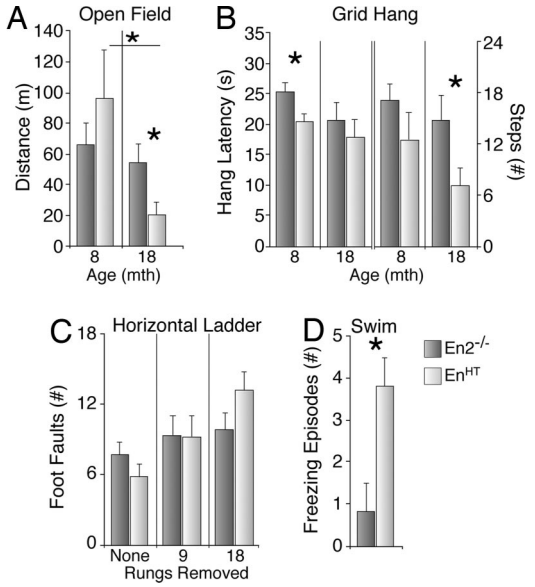

Fig. 4. Behavioral phenotype. (*A*) Open field test. *En1*+/−;*En2*−/− (*En*^{HT}) mice exhibited reduced locomotor activity at 18 mo of age, but not at 8 mo. (*B*) Grid hang test. Eight-month-old *En*^{HT} mice were not able to hang onto the mesh grid as long as their *En2*−/− counterparts (*Left*). Although this effect was less pronounced at 18 mo, at this age, the locomotor activity of *En*^{HT} mice was reduced by more than half (*Right*). (*C*) Horizontal ladder test. Although there were performance decrements as more rungs were removed, the performance of *En*^{HT} mice was not significantly impaired relative to *En2*−/− littermates. (*D*) Swimming test. *En*^{HT} mice exhibited four times more bouts of freezing than the controls ($n \geq 8$ for all tests). Error bars, standard deviation; *, $P < 0.05$.

showed a significant reduction in forward locomotion compared with *En2*−/− littermate controls (−63%; $P < 0.05$) and to their own performance at 8 mo (−79%; $P < 0.05$), whereas in *En2*−/− mice, locomotion was not significantly altered (−18%; Fig. 4*A*). In the grid/hang performance tests, which provides an index of motor strength in combination with locomotor ability, *En*^{HT} mice were able to hang from the inverted grid for a significantly shorter duration than their *En2*−/− littermate controls at 8 mo of age ($P <$ 0.05) and, although there was no significant difference in hang time at 18 mo of age, the number of steps they took while hanging was significantly reduced (−52%; $P < 0.05$) relative to *En2*−/− mice (Fig. 4*B*).

We did not observe significant differences between groups in the four remaining behavioral tests of motor coordination. The *En*^{HT} mice performed increasingly worse in the horizontal ladder test as more rungs were removed; however, their performance was not statistically different from that of *En2*−/− mice (Fig. 4*C*). Furthermore, although both groups showed a significant age-related decline in their ability to stay on the rotating spindle during the rotorod task, there were no between-group differences (data not shown). Finally, we found no differences between groups when we assessed rearing behavior in the cylinder task or measured forelimb and hindlimb stride lengths at either 8 or 18 mo of age (data not shown).

The performance of *En*^{HT} and *En2*−/− mice was also compared in two tests that provide indices of nonmotor behavior. We found no difference between or within groups across time in performance on the elevated plus maze, a measure of anxiety-related behavior. In the Morris water task, a test of spatial learning, 8 mo-old *En*^{HT} mice required significantly more time to find the hidden platform than their *En2*−/− littermates. However, we observed that the *En*^{HT} mice exhibited long periods of time when they would freeze in the water and just float. When

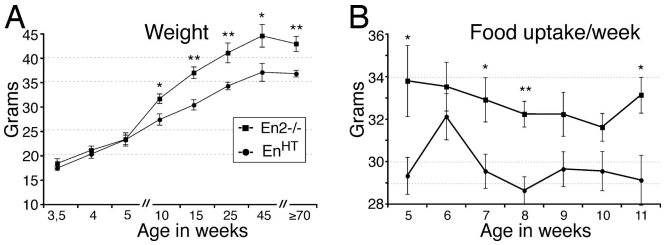

Fig. 5. Body weight and food uptake. Charts representing weight and food uptake in *En*^{HT} and *En2*−/− littermates over time. (*A*) *En*^{HT} mice are not subject to the same weight gains as their *En2*−/− littermate controls. The *x* axis is skewed toward the first postnatal weeks to emphasize difference between early postnatal and adult phases. (*B*) Weekly food uptake per mouse. *En*^{HT} mice eat significantly less per week than their littermate control. Each data point reflects the average from measurements of at least eight mice, sometimes up to 44. Error bars, standard error; *, $P < 0.01$; **, $P < 0.001$.

the animals were startled with an auditory stimulus each time they stopped swimming, *En*^{HT} and *En2*−/− littermate controls performed equally well (data not shown). To more specifically investigate this behavioral deficit, we examined the animal's swimming performance in a water-filled alley. Although we observed no asymmetries in paw use or differences in forepaw inhibition, *En*^{HT} mice exhibited four times as many episodes of freezing compared with *En2*−/− littermates (Fig. 4*D*).

Weight Reduction During Nigral Degeneration. Weight loss is a common feature among PD patients (6, 7). Although the cause is still debated, gastrointestinal dysfunction had been suggested due to the often-occurring degeneration of the enteric nervous system during disease progression (30). It is plausible, however, that the diminished DA innervation to the CPu is the cause for the weight loss, because patients with subthalamic deep-brain stimulation gain weight after onset of treatment (31, 32). To determine whether the degeneration of the nigrostriatal system in *En*^{HT} mice is accompanied by lower weight, we recorded the body weight of the mutants and their *En2*−/− littermate controls over their entire lifespan (Fig. 5). For the first 5–6 wk after birth, the weight was the same for both genotypes; however, thereafter the rate of weight gain slowed down in *En*^{HT} mice, and weight differences became apparent. From 15 weeks onward, *En*^{HT} mice weighed ≈16–20% less than their *En2*−/− littermate controls (80.2 ± 1.1%; $P = 0.001$ for 15-wk-old animals; Fig. 5*A*). To examine whether the weight disparity is caused by lower food uptake, we measured food consumption biweekly between 5 and 11 wk after birth. During this period, *En*^{HT} mice consumed significantly less food per day than the *En2*−/− controls (29.1 g ± 0.81 and 32.2 g ± 0.83, respectively; $P = 0.0031$; Fig. 5*B*). Because the lower weight uptake of *En*^{HT} animals is correlated to the loss of nigral DA neurons, and the *Engrailed* genes are not expressed by the enteric nervous system (20), it is likely that the lower weight of *En*^{HT} mutants is the result of the DA depletion in the CPu, but other causes cannot be excluded.

Discussion

We provide evidence that partial deletion of the *Engrailed* genes in mice leads to a selective and progressive degeneration of nigral DA neurons over the first 3 mo of their lives. This loss, which does not affect other DA groups in the mesencephalon, results in reduced storage and release of dopamine in the CPu, molecular changes in the GABAergic output neurons, motor deficits, and lower body weight. The phenotype of these mutant mice resembles key pathological features of PD.

Because *En*^{HT} mice are not the result of a genetic deletion targeted exclusively to mesDA neurons, it is possible that the deficiencies in other neuronal populations and not the reduced

dopamine signaling in the CPu causes the altered motor behavior and the weight loss. However, the options are limited. Because all results were obtained by a comparison between En^{HT} and *En2*−/− mice, it is unlikely that neurons expressing only *En2*, like the cerebellar granule cells, contribute to the phenotype (20). *En1* is expressed in the postnatal brain by a subset of Bergmann glia in the cerebellum, by radial glia in the ventral midbrain, and by undefined cell types in superior and inferior colliculus (9). Furthermore, it is transiently expressed by a subset of interneurons in the spinal cord (33), which control the speed of the vertebrate locomotor outputs. The latter could be a cause for the altered motor behavior; however, an *En1*-heterozygous phenotype was not been reported for these interneurons (19). Alternatively, the phenotype of En^{HT} mice could be linked to the early embryonic function of *En1*. It participates in the regionalization of the neural tube in a gene-dose-dependent manner during early embryogenesis, leading in *Engrailed* double mutant mice to different degrees of deletion in mid-/hindbrain tissue correlated to the allelic composition (34). The brain morphology of En^{HT} and *En2*−/− were not apparently different, and the number of noradrenergic neurons in the locus coeruleus was the same, suggesting that the phenotype of En^{HT} mice is not related to the early embryonic function of *En1*. However, this needs further investigation.

The specific loss of nigral DA neurons in En^{HT} mice during the first 3 postnatal mo is a unique feature not found in other genetic models for PD. In *Tgfα*-null mutants (35) and *Aphakia* (*Pitx3*−/−) mice (17), the loss is also specific to nigral DA neurons but occurs in the embryo and is already completed before birth. In *Weaver* mutant mice, a gain-of-function mutation of the inward-rectifying potassium channel *Girk2* (36) results in an unspecific opening of the channel and influx of sodium ions. In these animals, degeneration is a postnatal event but affects also VTA and RRF (37). In strong contrast to En^{HT} mutant mice, cell loss is also observed in other neuronal populations that express *Girk2*. For example, the cerebellar granule cells fail to differentiate and die before they migrate into deeper layers of the cerebellum (38). Despite strong expression of *En2* in granule cells, this cell population appears normal in En^{HT} mutants, with the exception of a small alteration in the organization of the cerebellar folia (28).

Adult En^{HT} mice exhibit a larger reduction in nigral DA neurons than idiopathic PD patients (39); however, their motor deficits are less severe. It is possible that significant differences in the neural circuits exist between rodents and humans, but alternatively, young mice may be able to activate compensatory mechanisms that are lost with age. This is supported by previous findings that young adult mice recover from 1-methyl-4-phenyl-1,3,6-tetrahydropyridine (MPTP) intoxication, whereas older animals do not (40). How the En^{HT} mice compensate for the loss of nigral DA neurons still needs to be addressed; however, the proportionally smaller reduction in dopamine content and release suggests that the remaining nigral DA neurons counteract the disappearance of their neighbors. On the other hand, the unexpected down-regulation of the *dopamine receptor 2* in the CPu, which is in contrast to the results obtained after acute experimental dopamine depletion (23), suggests that the adaptation could happen through changes in the GABAergic output neurons.

The loss of DA neurons in the SN but not in the VTA and the RRF, even though they all express the two *Engrailed* genes, indicates that the lowered *En1* expression in En^{HT} mice exposes a distinct vulnerability of nigral DA neurons. This vulnerability is likely an innate *Engrailed*-independent property of this cell population, because PD pathogenesis in the mesencephalon (41) and toxin-based experimental models also shows a preferential susceptibility to degeneration of nigral DA neurons (42). These similarities suggest that detailed examination of the underlying molecular mechanism that leads to the cell death in the *Engrailed* mutants could improve our understanding of the molecular etiology of PD.

Materials and Methods

Animals. The generation of the *En2*-null mutant and the *En1tau-LacZ* knockin mice were previously described (19, 43). In all experiments, the *En1*-null allele is *En1tau-LacZ*. The *En2* mutants with an original mixed genetic background of 129 and Swiss–Webster were crossed three times into a C57/BL6 background. The line was bred as *En1*+/*tlZ;En2*−/− at the central animal facility, University of Heidelberg.

Immunohistochemistry and *in Situ* Hybridization. All immunostainings and *in situ* hybridizations were performed as described (8, 9). The following additional antibodies were used: rabbit anti-glutamate decarboxylase 65 and 67 (Gad; AB1511) and rabbit antiglial fibrillary acidic protein (MAB360), both from Chemicon (Hampshire, U.K.).

Estimation of Cell Number in the Mesencephalon. To count TH-positive cells, a computer-assisted image system was used. The counting area was depicted at low magnification (×5), and SN, VTA, and RFF were separated by using exact anatomical criteria (12). These criteria can be imagined in a simplified but almost accurate manner by laying a line from the most lateral tip of the SN to the most ventral point of the midline of the brain section. Cells ventral to this line are counted as SN and in dorsal position as VTA. SN and RRF were distinguished by a morphological gap in rostral to caudal direction separating them. The number of TH-positive cells was estimated with an optical fractionator probe (Stereoinvestigator 5.04 MicroBrightField, Williston, VT). The settings were determined empirically; the grid size was set at 100 μm, and the sampling size was 30 × 30 μm. Sections were sampled with a frequency of 2. Coefficient of error (<0.1) was taken into account to validate each estimate. In the case of the noradrenergic neurons in the locus coeruleus and nucleus subcoeruleus, we did not estimate the numbers with the fractionator probe; instead, we blindly counted each cell.

HPLC. To measure the dopamine content, we dissected the dorsal striatum from the nucleus accumbens and olfactory tubercle and analyzed the tissue for dopamine content by reverse-phase HPLC, as described (44).

Quantitative RT-PCR. Quantitative RT-PCRs were performed with a 7000 Sequence Detection System from Applied Biosystems (Foster City, CA) by using preformulated assays on-demand and calculating the results with the comparative computed tomography method. The assays had the following identification tags: Mm00436880_m1 for *substance P*, Mm00438541_m1 for *dopamine receptor 2*, and Mm00457572_m1 for *dynorphin*; as standard control, Mm00507222_s1 *ribosomal protein S18*, Mm00435617_m1 for *phosphoglycerate kinase 1 (Pgk1)*, and Mm00446973_m1 for *TATA box-binding protein (Tbp)*. The dissected striata were homogenized and the RNA isolated and reverse-transcribed by using random hexamers to initiate transcription. Each individual PCR was done in three biological replicates, and at least two of three standard controls were run in parallel each time.

Fast-Scan Cyclic Voltametry in Brain Slices. DA overflow was measured in 300-μm-thick coronal striatal slices from En^{HT} mice and *En2*−/− controls (4–6 mo old). Animals were anesthetized with isoflurane and decapitated and the brains rapidly removed and kept in ice-cold high-magnesium artificial cerebrospinal fluid (aCSF) containing 124 mM NaCl, 3.3 mM KCL, 1.2 mM KH_2PO_4, 2.6 mM $MgSO_4$, 2.5 mM $CaCl_2$, 20 mM $NaHCO_3$, and 10 mM glucose, saturated with 95% O_2^- 5% CO_2. Slices were cut with a vibratome (Leica VT1000S, Nussloch, Germany) and kept after preparation at room temperature in normal magnesium aCSF (1.3 mM $MgSO_4$). Slices were then transferred to a

submerged recording chamber, where they were perfused at 2–3 ml/min aCSF at room temperature. DA release was evoked by a single pulse (0–500 μA, 300 μsec) applied through a bipolar stimulation electrode (bipolar stainless steel, 100 μm, insulated except at the tip) every 10 sec. DA was detected with 5-μm carbon-fiber electrodes (ALA Scientific Instruments, Westbury, New York) by using fast-scan cyclic voltametry (22). Cyclic voltamograms (ramps from -500 to $+1{,}000$ mV and back to -500 mV at 300 V per sec) were repeated every 100 ms by using an EPC9 amplifier (HEKA Electronic, Lambrecht, Germany). The background current obtained before release was subtracted from the current measured after release. The oxidation current of dopamine (between 500 and 700 mV) was converted to DA concentration by electrode calibration at the end of the experiment by using 0–10 μM DA as standards. Group averages were compared by using Student's t test.

Behavioral Studies. Except for the open-field and the water maze tests, behavioral activity was videotaped and analyzed by using video replay. Behavior in the open field and water maze tests was recorded and quantified by using an automated video tracking system. With the exception of the limb-use asymmetry and stride tests, behavioral testing was performed once per day for 5 days consecutively. All tests were performed during the animal's light cycle.

Open field test. A circular area (1.55-m diameter, 0.46-m high) constructed of white fiberglass served as the open field arena. The mice permitted to freely explore for 10 min while an image tracking system (HVS Image, Hampton, U.K.) recorded total distance traveled, average walking speed, and percent time spent in the central, intermediate, and peripheral regions. The arena was cleaned between trials with 70% ethanol and distilled water.

Swim task. Swimming behavior was assessed in a glass-fronted alley (1.2 m $\times$ 8.5 cm) filled with 21°C water to a depth of 43 cm. The mice were placed in one end of the alley, and their behavior was video-recorded as they swam to a wire-mesh exit ramp at the other end. Swim latency, limb-use asymmetry, episodes of forepaw disinhibition, and freezing behavior were quantified. Freezing was defined as motionless floating for a minimum duration of 3 sec.

Rotorod test. An automated rotorod (Rotomex Rotorod 950, Columbus Instruments, Columbus, OH) was used to assess motor coordination and balance. Mice were individually placed on the spindle, whereupon it began rotating at 6 rpm and accelerated linearly to 30 rpm over 2 min. The latency to fall off the rod was recorded.

The hang test, grid performance test, Morris water task, horizontal ladder test, stride length test, elevated plus maze, and cylinder task are described elsewhere (24–27, 45, 46).

Body Weight and Food Consumption. Male mice, which were provided with food ad libitum, were weighed at different ages after weaning until senescent ages (17 mo). The average and standard error were calculated for all groups of ages. For measuring food consumption, the animals were individually housed and the food pellets biweekly weighed.

Statistical Analysis. Values are expressed as mean $\pm$ standard error. Differences between means were analyzed by using a paired two-tailed Student's t test. For weight analysis, we performed Student's t test with two-sample equal variance (homeoscedastic) and one-tailed distribution. For motor performance tests, the null hypothesis was rejected at the 0.05 level and for all others, at the 0.01 level. All P values shown are rounded up at the third or fourth digit.

We thank Martyn Goulding (Salk Institute, La Jolla, CA) for the *En1/tauLacZ* and Alex Joyner (New York University School of Medicine, New York, NY) for the *En2* mutant mice and Marco Chiarandini and Tommaso Schiavinotto for help with the statistical analysis. We are particularly grateful to Andrew Lumsden and Peter Burbach for discussions on the manuscript. We also thank Gabriele Döderlein, Richard Hertel, Kendra Laustsen, and Rae Kokotailo for technical assistance. This work was supported by grants from the Federal Secretary for Education and Research (BMBF) Biofuture 98; the Michael J. Fox Foundation; the National Parkinson Foundation (to H.H.S.); the Canadian Institutes of Health Research; and the Natural Sciences and the Engineering Research Council of Canada (to R.H.D.).

1. Fallon JH, Loughlin SE (1994) in *The Rat Nervous System*, ed Paxinos G (Academic, London), pp 215–237.
2. Schultz W (2002) *Neuron* 36:241–263.
3. Girault JA, Greengard P (2004) *Arch Neurol* 61:641–644.
4. Eells JB (2003) *Curr Med Chem* 10:857–870.
5. Olanow CW, Tatton WG (1999) *Annu Rev Neurosci* 22:123–144.
6. Beyer PL, Palarino MY, Michalek D, Busenbark K, Koller WC (1995) *J Am Diet Assoc* 95:979–983.
7. Chen H, Zhang SM, Hernan MA, Willett WC, Ascherio A (2003) *Ann Neurol* 53:676–679.
8. Alberi L, Sgadò P, Simon HH (2004) *Development (Cambridge, UK)* 131:3229–3236.
9. Simon HH, Saueressig H, Wurst W, Goulding MD, O'Leary DD (2001) *J Neurosci* 21:3126–3134.
10. Hanks M, Wurst W, Anson-Cartwright L, Auerbach AB, Joyner AL (1995) *Science* 269:679–682.
11. West MJ (1993) *Neurobiol Aging* 14:275–285.
12. German DC, Manaye KF (1993) *J Comp Neurol* 331:297–309.
13. Oo TF, Kholodilov N, Burke RE (2003) *J Neurosci* 23:5141–5148.
14. Simon HH, Thuret S, Alberi L (2004) *Cell Tissue Res* 318:53–61.
15. Burke RE, Antonelli M, Sulzer D (1998) *J Neurochem* 71:517–525.
16. Smidt MP, Asbreuk CH, Cox JJ, Chen H, Johnson RL, Burbach JP (2000) *Nat Neurosci* 3:337–341.
17. Smidt MP, Smits SM, Bouwmeester H, Hamers FP, Van Der Linden AJ, Hellemons AJ, Graw J, Burbach JP (2004) *Development (Cambridge, UK)* 131:1145–1155.
18. McCaffery P, Drager UC (1994) *Proc Natl Acad Sci USA* 91:7772–7776.
19. Saueressig H, Burrill J, Goulding M (1999) *Development (Cambridge, UK)* 126:4201–4212.
20. Davis CA, Joyner AL (1988) *Genes Dev* 2:1736–1744.
21. Davis CA, Holmyard DP, Millen KJ, Joyner AL (1991) *Development (Cambridge, UK)* 111:287–298.
22. Kawagoe KT, Zimmerman JB, Wightman RM (1993) *J Neurosci Methods* 48:225–240.
23. Gerfen CR (2000) *Trends Neurosci* 23:S64–S70.
24. Tillerson JL, Miller GW (2003) *J Neurosci Methods* 123:189–200.
25. Tillerson JL, Caudle WM, Reveron ME, Miller GW (2002) *Exp Neurol* 178:80–90.
26. Metz GA, Whishaw IQ (2002) *J Neurosci Methods* 115:169–179.
27. Fernagut PO, Diguet E, Labattu B, Tison F (2002) *J Neurosci Methods* 113:123–130.
28. Millen KJ, Wurst W, Herrup K, Joyner AL (1994) *Development (Cambridge, UK)* 120:695–706.
29. Gerlai R, Millen KJ, Herrup K, Fabien K, Joyner AL, Roder J (1996) *Behav Neurosci* 110:126–133.
30. Pfeiffer RF (2003) *Lancet Neurol* 2:107–116.
31. Macia F, Perlemoine C, Coman I, Guehl D, Burbaud P, Cuny E, Gin H, Rigalleau V, Tison F (2004) *Mov Disord* 19:206–212.
32. Barichella M, Marczewska AM, Mariani C, Landi A, Vairo A, Pezzoli G (2003) *Mov Disord* 18:1337–1340.
33. Gosgnach S, Lanuza GM, Butt SJ, Saueressig H, Zhang Y, Velasquez T, Riethmacher D, Callaway EM, Kiehn O, Goulding M (2006) *Nature* 440:215–219.
34. Simon HH, Scholz C, O'Leary DD (2005) *Mol Cell Neurosci* 28:96–105.
35. Blum M (1998) *Nat Neurosci* 1:374–377.
36. Roffler-Tarlov S, Martin B, Graybiel AM, Kauer JS (1996) *J Neurosci* 16:1819–1826.
37. Gaspar P, Ben Jelloun N, Febvret A (1994) *Neuroscience* 61:293–305.
38. Harkins AB, Fox AP (2002) *Cerebellum* 1:201–206.
39. Dunnett SB, Bjorklund A (1999) *Nature* 399:A32–9.
40. Ricaurte GA, DeLanney LE, Irwin I, Langston JW (1987) *Neuropharmacology* 26:97–99.
41. Damier P, Hirsch EC, Agid Y, Graybiel AM (1999) *Brain* 122 (Pt 8):1437–1448.
42. Dauer W, Przedborski S (2003) *Neuron* 39:889–909.
43. Joyner AL, Herrup K, Auerbach BA, Davis CA, Rossant J (1991) *Science* 251:1239–1243.
44. Wachtel SR, Bencsics C, Kang UJ (1997) *J Neurochem* 69:2055–2063.
45. Sutherland RJ, Dyck RH (1984) *Can J Psychol* 38:322.
46. Schallert T, Fleming SM, Leasure JL, Tillerson JL, Bland ST (2000) *Neuropharmacology* 39:777–787.